Dyes and Pigments 101 (2014) 109–115

Contents lists available at ScienceDirect

Dyes and Pigments

journal homepage: www.elsevier.com/locate/dyepig

Fluorescence response of pyridinyl- and/or dibutylaniline-capped 2,6,9,10-tetravinylanthracenes to metal ions

Meng Zheng, Mingxiao Sun, Deteng Zhang, Tongliang Liu, Shanfeng Xue, Wenjun Yang*

Key Laboratory of Rubber-Plastics of Ministry of Education (QUST), School of Polymer Science & Engineering,
Qingdao University of Science & Technology, 53, Zhengzhou Road, Qingdao 266042, China

A R T I C L E I N F O

Article history:
Received 16 July 2013
Received in revised form
9 September 2013
Accepted 11 September 2013
Available online 6 October 2013

Keywords:
Anthracene-centered cruciform
Intramolecular charge transfer
Chemosensor
Transition metal ion
Frontier molecular orbital
Fluorescence responsive behaviors

A B S T R A C T

The solution photophysical properties of a series of dibutylaniline- and/or pyridine-containing 2,6,9,10-tetrarylvinylanthracene cruciforms with and without metal ions have been determined. The results show that the dibutylaniline-containing cruciforms show stronger intermolecular charge transfer and obviously red-shifted emission spectra than the only pyridine-containing ones, and fluorescence responses of these cruciforms to select several metal ions are also different. The alkali K^+, alkaline-earth Mg^{2+} and Ca^{2+} hardly affect the emission behavior, but the transition Cu^{2+} and Zn^{2+} could red-shift, blue-shift or quench the fluorescence emissions, depending on the nature of end groups. The fluorescence responsive behaviors of the different cruciforms to metal ions are explained qualitatively through their spatially separated frontier molecular orbital (FMO) features and coordination-induced FMO changes. These findings suggest that these anthracene-centered cruciforms could be promising functional scaffolds selectively for differential transition metal sensor arrays.

1. Introduction

Most organic chromophores exhibit spatially superimposed HOMO and LUMO. However, when center-crossed two-dimensional (2-D) conjugated molecules with an aromatic ring as the common π-center (named cruciform) are added donor and/or acceptor terminals, independent electronic shifts into opposite directions in HOMO and LUMO could be attained [1–8]. Generally, the HOMO is located on the electron-rich (or donor-containing) branch, while the LUMO is situated on the electron-deficient (or acceptor-incorporating) axis of molecule. As a result, the intramolecular charge transfer absorption and emission properties of such cruciform are dependent on both their structures and chemical environments [9–16], to render them unique and interesting optical and optoelectronic properties. For example, 1,2,4,5-tetrasubstituted benzene-centered cruciform with dibutylamine and/or pyridine end-groups show dramatic blue and/or red shifts of emission and absorption upon coordination of metal cations, which have been regarded as valuable functional scaffolds for differential metal sensor arrays [1,16–22].

We have been interested in anthracene-centered linear and 2-D fluorophore cruciforms because of their unique structures and interesting optical properties that are different from benzene-centered cruciforms [23–28]. For instance, 2,6,9,10-tetrasubstituted anthracene-centered cruciforms are non-centrosymmetric chromophores and show enhanced two-photon absorption effect [24,25], however, the centrosymmetric benzene- or pyrazine-based cruciforms do not exhibit the enhanced two-photon absorption (2PA) cross sections [26–28]. Also, some cruciforms have potential applications for the molecular electronics [29–31] and the construction of functional scaffolds for differential amine sensor arrays [15,16,32–34]. These results imply that different types of π-centers and molecular symmetry could endow cruciforms with different optical properties and applications. In the previous works, we have reported the one- and two-photon absorption and excitation fluorescence properties of several anthracene-centered cruciforms and 2-D cross-conjugated polymers [24,25,35]. Motivated to further understand of anthracene-centered cruciforms' optical properties and develop their applications, we have recently designed and synthesized a new series of 2,6,9,10-tetra(arylvinyl)anthracene cruciforms with dibutylaniline and/or pyridine as the end groups, and their aggregation-enhanced one- and two-photon excitation fluorescence properties have been investigated [35]. It is known that pyridine and dibutylaniline

---

* Corresponding author. Tel.: +86 532 84023670; fax: +86 532 84023977.
E-mail address: ywjph2004@qust.edu.cn (W. Yang).

0143-7208/$ – see front matter © 2013 Elsevier Ltd. All rights reserved.
http://dx.doi.org/10.1016/j.dyepig.2013.09.037

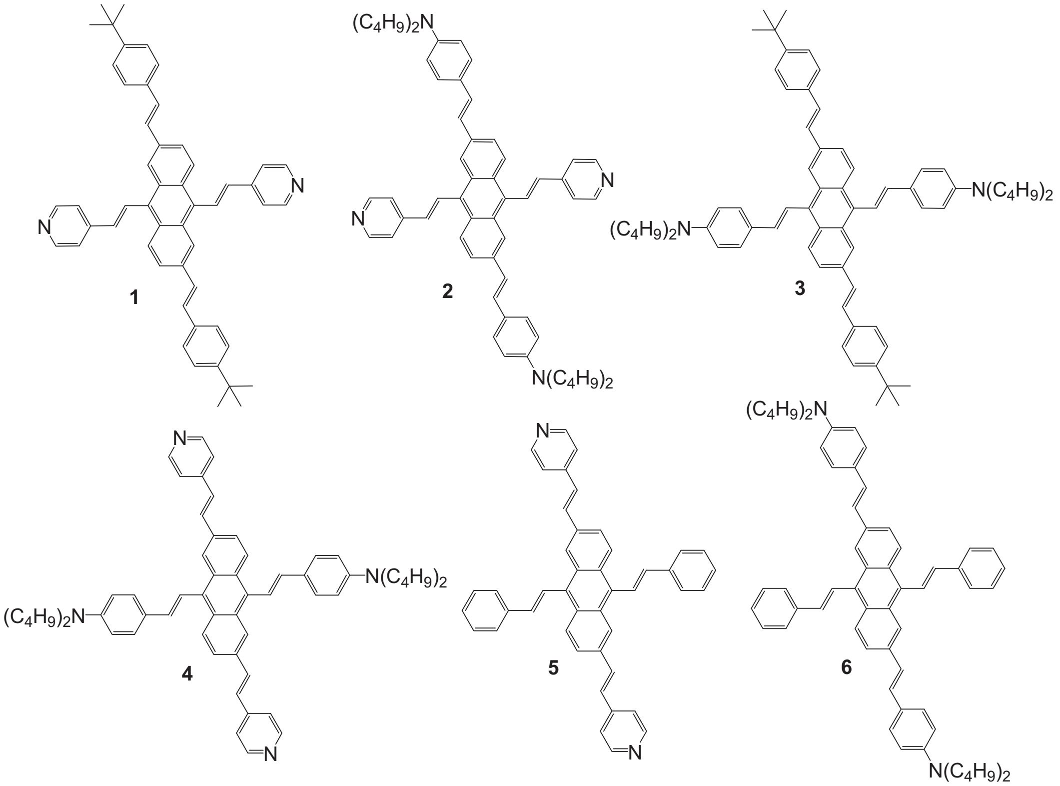

Fig. 1. Chemical structures of dibutylaniline and/or pyridine-capped 2,6,9,10-tetravinylanthracene cruciforms **1**–**6**.

moieties have coordination potential with metal cations because of the existence of lonely electronic pairs at nitrogen, and the donor/acceptor-substituted anthracene-centered cruciforms have been characteristic of spatially separated HOMO and LUMO. Therefore, it is necessary to examine the fluorescence sensing properties of these anthracene-centered cruciforms to metal cations. Here we have prepared six permutations of the donor- and/or acceptor-containing tetrakis(arylvinyl)anthracenes (Fig. 1), and several different physiologically active metal cations (alkali K^+, alkaline-earth Mg^{2+} and Ca^{2+}, and transition Cu^{2+} and Zn^{2+}) are chosen as examples [36–40], which should permit a more systematic investigation on the effect of structural variations (nature and position of donor/acceptor moieties) and metal ions on the absorption and emission properties. For the sake of comparison, the parent cruciform, 2,6-bis(*p*-*tert*-butylstyryl)-9,10-bis(styryl)anthracene (**PC**, Scheme 1) is also included.

2. Experimental section

2.1. Materials

Triethylamine (NEt_3) over calcium hydride and tetrahydrofuran over metallic sodium were distilled before use. 4-pyridylaldehyde, triflates of Zn^{2+}, Cu^{2+}, Mg^{2+}, Ca^{2+}, and K^+ were commercially available from Energy Chem. Co. Ltd., China. Other solvents and reagents were analytical grade and used as received without further purification. Cruciforms **1**–**5** and **PC**, 2,6-bis(diethylphosphorylmethyl)-9,10-dibromoanthracene and 4-dibutylaminobenzaldehyde were from the previous work [35].

2.2. Synthesis of 2,6-bis(diethylphosphorylmethyl)-9,10-distyrylanthracene

A pressure tube containing a mixture of styrene (0.37 g, 3.6 mmol), 2,6-bis(diethylphosphorylmethyl)-9,10-dibromoanthracene (0.45 g, 0.71 mmol), $Pd(OAc)_2$ (15 mg, 0.067 mmol), tris(*o*-tolyl)phosphine (0.13 g, 0.42 mmol), $N(C_2H_5)_3$ (3 mL) and THF (3 mL) was sealed under nitrogen and refluxed at 80 °C for 24 h. The mixture was separated by a column chromatography on silica gel using ethyl acetate/hexane (3/1) as the eluent. Yield: 0.35 g (73%). ^1H NMR (500 MHz, $CDCl_3$):δ 8.36 (d, 2H), 8.21 (s, 2H), 7.90 (d, 2H), 7.70 (d, 4H), 7.48 (m, 6H), 7.39 (m, 2H), 6.94 (d, 2H), 4.03 (m, 8H), 3.33 (d, 4H), 1.23 ppm (m, 12H). Anal. Calcd. for $C_{40}H_{44}O_6P_2$: C, 70.37; H, 6.50; O, 14.06; P, 9.07. Found: C, 70.46; H, 6.47.

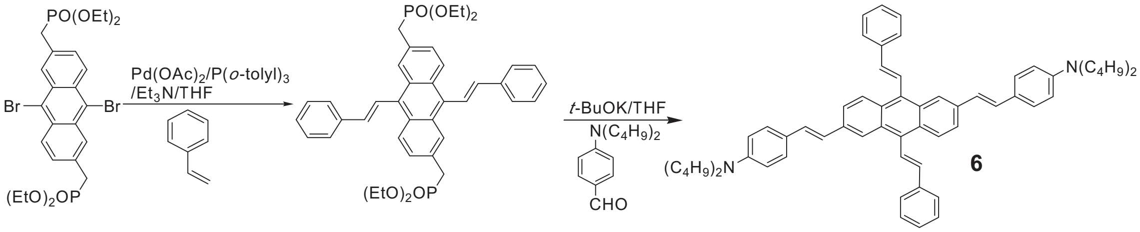

Scheme 1. The synthesis and structure of cruciform **6**.

2.3. Synthesis of 2,6-bis(4-dibutylaminostyryl)-9,10-distyrylanthracene (**6**)

Potassium *t*-butoxide (0.16 g, 1.43 mmol) was added to the mixture of 2,6-bis(diethylphosphorylmethyl)-9,10-distyrylanthracene (0.13 g, 0.19 mmol) and 4-dibutylaminobenzaldehyde (0.13 g, 0.56 mmol) in anhydrous THF (15 mL) at room temperature under N_2. The mixture was stirred overnight and then 100 mL of methanol was added. The precipitate was collected and purified by a column chromatography on silica gel using hexane/dichloromethane (2/1) as the eluent. Yield: 91 mg (57%). ^{1}H NMR (500 MHz, $CDCl_3$) δ (ppm): 8.32 (d, 2H), 8.17 (s, 2H), 7.92 (d, 2H), 7.75 (m, 6H), 7.51 (m, 4H), 7.42 (m, 6H), 7.11 (m, 4H), 6.98 (d, 2H), 6.63 (d, 4H), 3.30 (t, 8H), 1.59 (m, 8H), 1.37 (m, 8H), 0.97 (m, 12H). ^{13}C NMR (125 MHz, $CDCl_3$): δ (ppm) 147.9, 137.3, 134.9, 134.5, 132.2, 130.8, 129.3, 128.9, 128.2, 128.0, 127.9, 127.0, 126.7, 125.4, 124.4, 124.1, 122.6, 118.6, 111.7, 50.8, 29.5, 20.4, 14.1. Anal. Calcd. for $C_{62}H_{68}N_2$: C, 88.52; H, 8.15; N, 3.33. Found: C, 88.41; H, 8.19; N, 3.37.

2.4. Measurements

UV–vis absorption spectra were recorded on a Hitachi U-4100 spectrophotometer. Fluorescence spectra were measured on a Hitachi F-4600 spectrophotometer, and the peak wavelength of the lowest energy absorption band was used as the excitation wavelength. The fluorescence quantum yield was determined by the literature method using rhodamine B as the reference [41]. The uncertainty for measured UV or PL is <2%. NMR spectra were recorded on an AVANCE 500 (Bruker) spectrometer in $CDCl_3$ with tetramethylsilane (TMS) as an internal standard. The elemental analysis was performed on Perkin–Elmer 2400. Metal ion coordination to cruciforms **1**–**6** was performed in dichloromethane (DCM, analytical grade). 5–60 μL of triflate salt (10^{-2} M in DCM) was respectively added to the solutions of **1**–**6** (5 mL, ~10^{-5} M in DCM) in a 10 mL of sample bottle via microsyringe to afford the cruciform solution with different equiv of metal ions. The resulting solutions were capped and shaken for 1 min and transferred into the four-sided quartz spectrophotometry cuvette. The fluorescence spectra were measured at room temperature.

3. Results and discussion

3.1. Synthesis

Donor and/or acceptor-capped anthracene-centered cruciforms presented here are the π-systems in which the 2,6- and 9,10-positions of a central anthracene ring are linked respectively with two different arylvinyl arms. Since anthracene is a non-centrosymmetric aromatic ring, 2,6,9,10-tetraarylvinylanthracenes have twice (six) as many permutations as benzene-centered analogues (three). The syntheses of **1**–**5** and **PC** have been described elsewhere [35], and the preparation of **6** is depicted in Scheme 1. The general synthetic route to **1**–**6** and **PC** starts from 2,6-bis(diethylphosphorylmethyl)-9,10-dibromoanthracene, which is first subjected to a Heck coupling with arylvinylenes (styrene, 4-dibutylaminostyrene, and 4-vinylpyridine), then followed by a Wittig–Horner reaction with 4-*tert*-butylbenzaldehyde, 4-pyridylaldehyde, and 4-dibutylaminobenzaldehyde to produce desirable cruciforms in good yields and purity after purification by a column chromatography on silica gel. Their structures and compositions have been unambiguously characterized by ^{1}H and ^{13}C NMR and element analysis.

3.2. Spectroscopic properties of the cruciforms **1**–**6** and **PC** in dichloromethane

The normalized absorption and emission spectra for cruciforms **1**–**6** and **PC** in dichloromethane (DCM) are displayed in Fig. 2, and the peak wavelengths of lowest-energy absorption brand (λ_{max}) and emission spectra (λ_{em}) are summarized in Table 1. The λ_{max} and λ_{em} of parent cruciform **PC** are 433 and 536 nm, respectively. When phenyl units at 2,6- or 9,10-positions are replaced by pyridine unit, the resulting cruciforms only show the slightly red-shifted λ_{max} (436 nm for **1**, and 438 nm for **5**), implying pyridine unit is a weak electron-withdrawing moiety. However, when phenyl units at 2,6- or 9,10-positions are changed into dibutylaniline units, significantly bathochromic shifted λ_{max} are observed (Fig. 2a and Table 1), indicating that dibutylaniline unit is a strong electron-donating moiety. Moreover, the λ_{max} of **2**, and **6** are longer than those **3**, and **4**, implying the intramolecular charge transfer (ICT) effect induced by dibutylamine unit at 2,6-positions is stronger than that at 9,10-positions, which could be ascribed to their different conjugation pathways and utility of resonance energy. Overall, there is a significant ICT effect between 9,10- and 2,6-branches for all the dibutylamine-containing cruciforms.

The λ_{em} of **PC** is at 540 nm, and only pyridine-containing cruciforms **1** and **5** show the moderately red-shifted λ_{em} (22, and 7 nm, respectively) due to the weak ICT effect (Fig. 2b, and Table 1). However, significantly red-shifted fluorescence emission (33–73 nm) are observed for those dibutylamine-containing cruciforms because of their stronger ICT effect that decreases energy gaps between the ground and Franck–Condon states. Although cruciforms **1**–**6** and **PC** are all 9,10-di(arylvinyl)anthracene-containing derivatives and have similar conjugation skeleton, dibutylamine-containing cruciforms show very low fluorescence quantum yields (Φ) (Table 1). These low Φ could be ascribed to the lower energy of the emitting states and/or the free intramolecular torsional motion of severely distorted 9,10-diarylvinyl moieties facilitated by the flexible dibutylamino moieties. It is observed that the λ_{em} of donor–acceptor-substituted cruciforms are longer than that of only donor-containing cruciforms, that is, **2** > **6**, **4** > **3**, implying that the weak acceptor could still stabilize the emitting states. Moreover, obviously red-shifted emissions for 9,10- over 2,6-dibutylamino-contaning cruciforms are observed, i.e. **4** > **2**, **3** > **6**, although their λ_{max} are in the opposite order, **2** > **4**, **6** > **3**. This indicates that dibutylamine linked at 9,10-positions could stabilize the emitting states more than that at 2,6-positions. As a sequence, the fluorescence Stokes shifts of cruciforms **3** and **4** are larger than those of cruciforms **2** and **6** and others (Table 1).

3.3. Fluorescence responses of **1**–**6** to select metal cations in DCM

Since pyridine- and/or dibutylaniline-capped benzene-centered cruciforms have been used as functional scaffolds for differential metal sensor arrays, it is interesting to examine the fluorescence response of anthracene-centered cruciforms **1**–**6** to metal ions. Here we have chosen several different physiologically-active metal cations (triflates of alkali K^+, alkaline-earth Mg^{2+} and Ca^{2+}, and transition Cu^{2+} and Zn^{2+}) as examples to investigate the effect of metal ions on emission properties of cruciforms **1**–**6** in DCM. Fig. 3 shows the fluorescence images of cruciforms **1**–**6** upon addition of an excess of metal ions (6 equiv). It is observed that there are no changes in fluorescence colors for these cruciforms upon addition of K^+, Mg^{2+}, and Ca^{2+} (Fig. 3a), indicating that these cruciforms have no sensing ability to the selected alkali and alkaline-earth metal ions, probably due to their weak coordination abilities each other. However, three kinds of different fluorescence responses are observed upon addition of Cu^{2+} or Zn^{2+} (Fig. 3b): (a) bathochromic

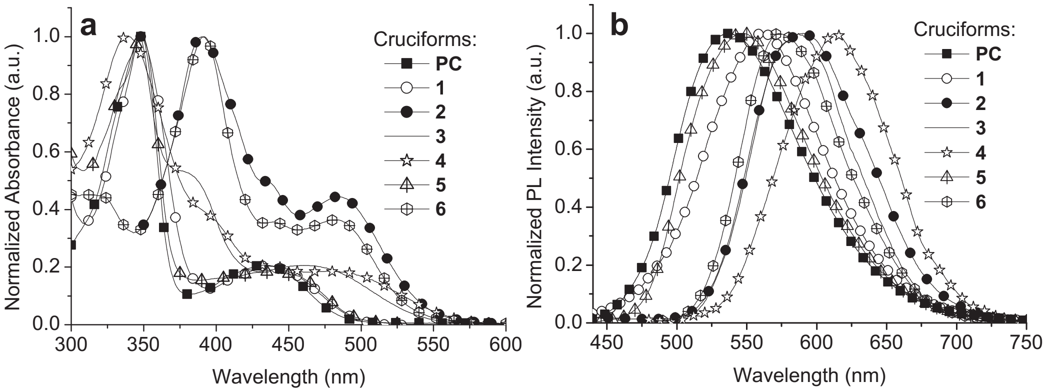

Fig. 2. Absorption and emission spectra of cruciforms **1**–**6** and **PC** in DCM at 1.0 × 10^{-5} M.

shifted emissions for **1** and **5** with Zn^{2+}, (b) hypsochromic shifted emissions for **2**, **3**, **4** and **6** with Zn^{2+} or for **3** and **6** with Cu^{2+}, and (c) quenched fluorescence for **1**, **2**, **4** and **5** with Cu^{2+}. It is noted that all the pyridine-containing cruciforms show quenched fluorescence upon the addition of Cu^{2+}. This implies that the interaction between Cu^{2+} and pyridine moiety could lead to fast non-radioactive decay of the excited states of these cruciforms, which is probably related to the electronic structure of Cu^{2+}. However, the real origin for this difference between Cu^{2+} and Zn^{2+} is unclear, and further investigations are needed. Nevertheless, Cu^{2+}, and Zn^{2+} can be distinguished from each other through these cruciforms. Their features are that single member of such a family do not well-recognize a specific analyse, but an ensemble of different ones will work. These findings suggest that cruciforms **1**–**6** could be regarded as a new family of differential sensor arrays selectively for transition metal ions.

The emission spectra of cruciforms **1**–**6** upon addition of 6 equiv of Cu^{2+} or Zn^{2+} are depicted in Fig. 4, and the relative spectroscopic data are summarized in Table 2. It is shown that Cu^{2+} can quench the fluorescence emissions of all the pyridine-containing cruciforms and blue-shift the emission spectra of only dibutylaniline-containing cruciforms (**3** and **6**). In contrast, Zn^{2+} does not quench the emission spectra of any cruciforms. Zn^{2+} can blue shift the emission spectra and enhanced the Φ of cruciforms **2**, **3**, **4** and **6**, but red-shift the emission spectra and decrease the Φ of cruciforms **1** and **5**. These changed emissions and Φ could be explained in terms of their frontier molecular orbital (FMO) features and fluctuations in energy levels upon coordination with metal ions (*vide infra*).

To gain further understanding of the impact of transition metal ions on the fluorescence behavior, cruciforms **3** and **4** are used as the representatives to be added different equiv of Cu^{2+} and Zn^{2+}, respectively. As shown in Fig. 5, their emission spectra are monotonously blue shifted with the increase of metal ions and then remain almost unchanged at high concentrations of metal ions. The monotonous spectral shift of cruciform **3** is understandable since it contains only one coordination axis. However, cruciform **4** with two different coordination axes exhibits still the monotonous spectral shift upon titration of metal ions, which requires further explanation since this phenomenon is different from that observed in the benzene-centred analogues whose spectral response to metal ions are generally two-stage (stepwise) [20,42]. Benzene ring is a real centrosymmetric π-center and its two ICT pathways are less twisted and more straight, which makes the coordination ability of two branches depend on predominately the nature of end functional groups. To our cruciforms, anthracene ring is an asymmetric π-center and the 9,10- and 2,6-ICT pathways are very different, one is zigzag (2,6-direction) and another is seriously twisted (9,10-direction). This could reduce the difference of coordination abilities between the two axes; moreover, the 2,6-zigzag and 9,10-twisted ICT pathways should weaken their coordination abilities to metal ions. This is possibly the reason why anthracene-centered cruciforms have no sensing ability to the alkali and alkaline-earth ions such as K^{+}, Mg^{2+}, and Ca^{2+}. On considering that the main difference between the benzene- and anthracene-centered cruciforms is the π-center, it could be concluded that the different type of π-center and molecular symmetry might endow the cruciforms with different optical properties and practical applications. It could be expected that changing the terminal recognition elements would lead to cruciforms with further enhanced and differentiated response capabilities, which is underway in our laboratory.

Table 1
Spectroscopic data of cruciforms **1**–**6** and **PC** in DCM at 1.0 × 10^{-5} M.

Cpd	PC	1	2	3	4	5	6
λ_{max}/nm[a]	435	439	484	466	474	440	479
λem/nm[b]	540	562	591	587	613	547	573
$\Delta\nu$/nm[c]	105	123	107	121	139	107	94
Φ[d]	0.61	0.50	0.037	0.045	0.049	0.42	0.15

[a] Peak wavelength of the lowest energy absorption band.
[b] Peak wavelength of emission spectra.
[c] Fluorescence stokes shift.
[d] Fluorescence quantum yield.

3.4. FMO features and coordination-induced fluctuations

Organic chromophores with disjoint frontier molecular orbital (FMO) features are promising materials in optical and optoelectronic fields but still quite rare. Therefore, it is very interesting to know the FMO features of functional anthracene-centerd cruciforms presented here and the changes in the energy level caused by metal ions. The HOMO and LUMO features of cruciforms **1**–**6** and **PC** calculated with B3LYP/6-31G* are depicted in Fig. 6. The LUMO of **PC** is very similar to its HOMO (Fig. 6a). **PC** shows spatially superimposable or congruent FMOs as a result of the lack of donor and/or acceptor end groups. However, when the phenyl units are replaced with dibutylaniline and/or pyridine moieties, the resulting cruciforms **1**–**6** all exhibit the spatially separated or disjoint FMOs with the central anthracene ring acting as an integral part of both orbital, regardless of the nature and linking positions of donor/acceptor units (Fig. 6b). Moreover, the HOMO density is always located on the dibutylaniline-containing branch, and LUMO density lies on invariably the pyridine-containing axis.

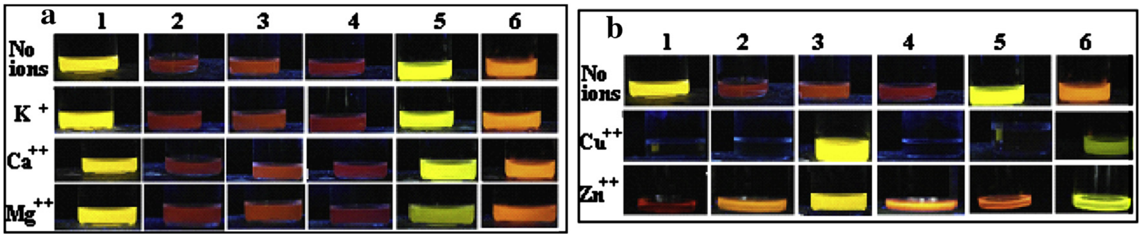

Fig. 3. Fluorescence images of cruciforms **1**–**6** in DCM at 1.0 × 10^{-5} M upon adding 6 equiv of metal ions under illumination with a 365 nm UV lamp. (For interpretation of the references to color in this figure legend, the reader is referred to the web version of this article.)

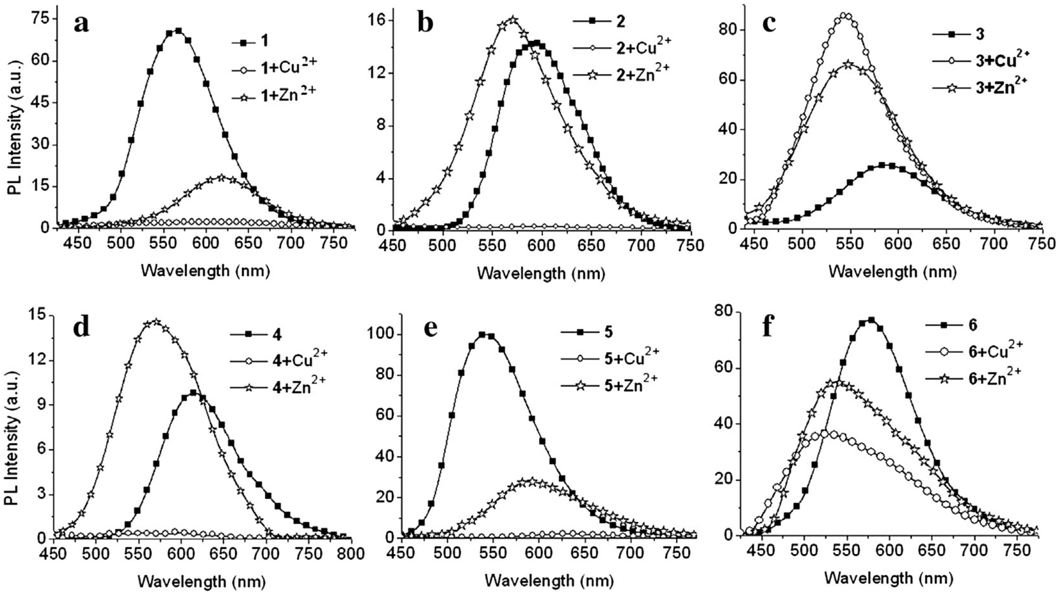

Fig. 4. Emission spectra of cruciforms **1**–**6** in DCM at 1.0 × 10^{-5} M upon adding 6 equiv of Zn^{2+} and Cu^{2+}.

It has been observed that cruciform **1** and **5** show bathochromic shifts and **2** and **4** hypsochromic shifts upon coordination with Zn^{2+}, and **3** and **6** show blue shifts upon coordination with both Zn^{2+} and Cu^{2+}. These fluorescence responses to metal ions can be rationalized by qualitatively examining relative energy levels of the FMOs as the coordination happens (Fig. 7.). In cruciform, pyridine and dibutylaniline act as an electron-withdrawing and an electron-donating group, respectively. Upon coordination with metal ions, the interaction between pyridine units and metal ions will enhance the electron-withdrawing ability of pyridine, and the coordination between dibutylaniline units and metal ions will weaken the electron-donating ability of dibutylamino. Thus, the coordination will lower the LUMO levels of only pyridine-containing cruciforms **1** and **5** (stabilizing the excited states), while the HOMO will not be greatly affected because it is situated on the non-coordinating distyrylanthracene branches of the cruciforms (Fig. 7a). The narrowed band-gaps will red-shift the emission spectra and decrease the Φ due to the lower energy of the emitting states that facilitate the non-radioactive pathways. In contrast, the coordination will lower the HOMO levels of only dibutylaniline-containing cruciforms **3** and **6** (stabilizing the ground states), while the LUMO will not be greatly affected because it is located on the distyrylanthracene arms without coordination ability (Fig. 7b). In this case, the band-gaps were broadened, blue-shifted emission spectra and increased Φ values were observed. For cruciforms **2** and **4** with donor–acceptor substituted motif, upon addition of Zn^{2+}, the coordination will lower both the HOMO situated on dibutylaniline-containing branch and the LUMO located on pyridine-containing arms (Fig. 7c). Since the emission spectra are blue-shifted and Φ increased upon coordination, the lowering extent of HOMO should

Table 2
Peak emission wavelengths and fluorescence quantum yields of cruciforms **1**–**6** in DCM at 1.0 × 10^{-5} M upon adding 6 equiv of Zn^{2+} and Cu^{2+}.

Cruciforms	1	2	3	4	5	6
λ_{em} (no ions)	562	591	587	613	547	573
Φ (no ions)	0.50	0.037	0.045	0.049	0.42	0.15
λ_{em} (+Zn^{2+})	620	569	548	568	579	526
Φ (+Zn^{2+})	0.045	0.072	0.26	0.11	0.089	0.21
λ_{em} (+Cu^{2+})	Not recorded	Not recorded	543	Not recorded	Not recorded	518
Φ (+Cu^{2+})	Quenched	Quenched	0.37	Quenched	Quenched	0.11

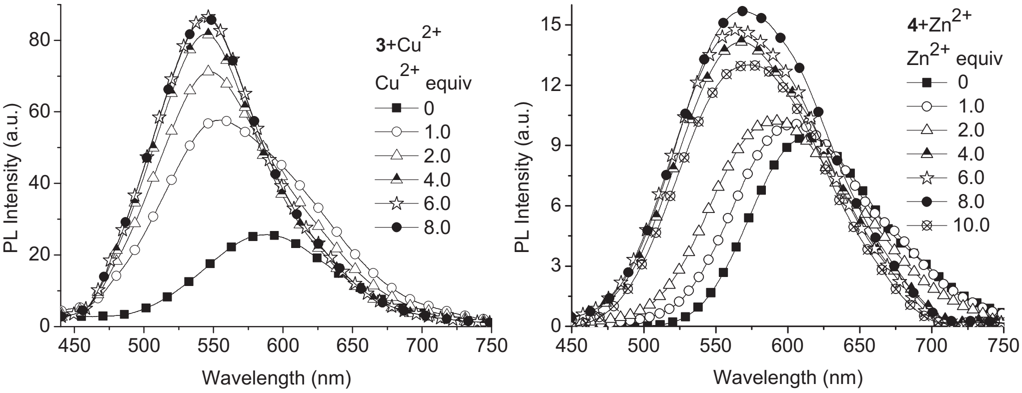

Fig. 5. Emission spectra of cruciforms **3** and **4** in DCM at 1.0 × 10^{-5} M upon titration of Cu^{2+} and Zn^{2+}, respectively.

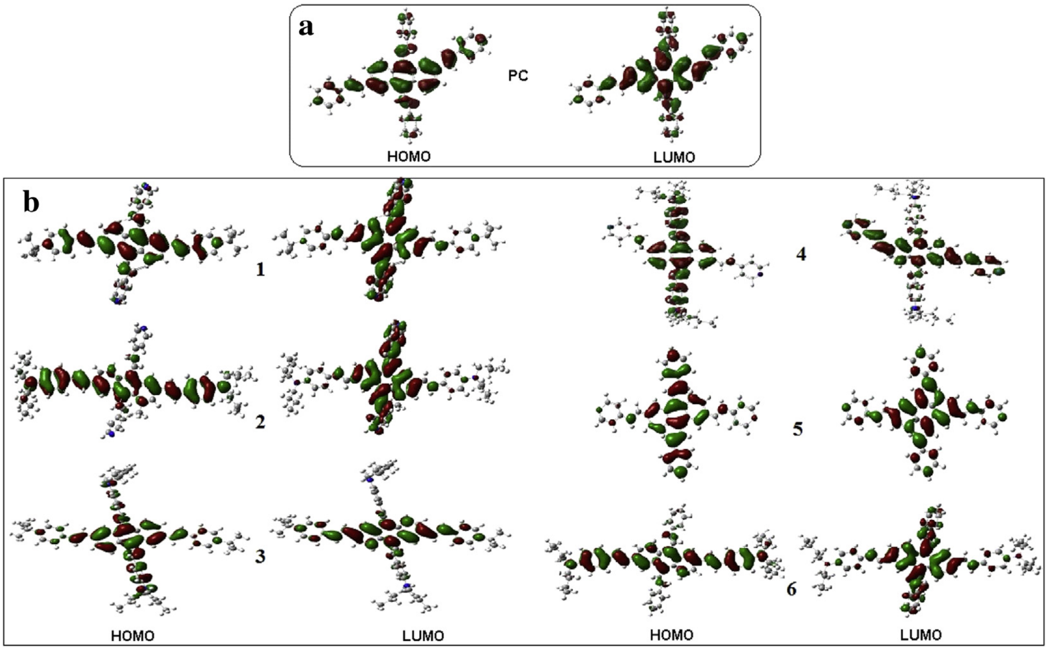

Fig. 6. Frontier molecular orbital plots of cruciforms **1**–**6** and parent **PC** calculated with B3LYP/6-31G* using Spartan.

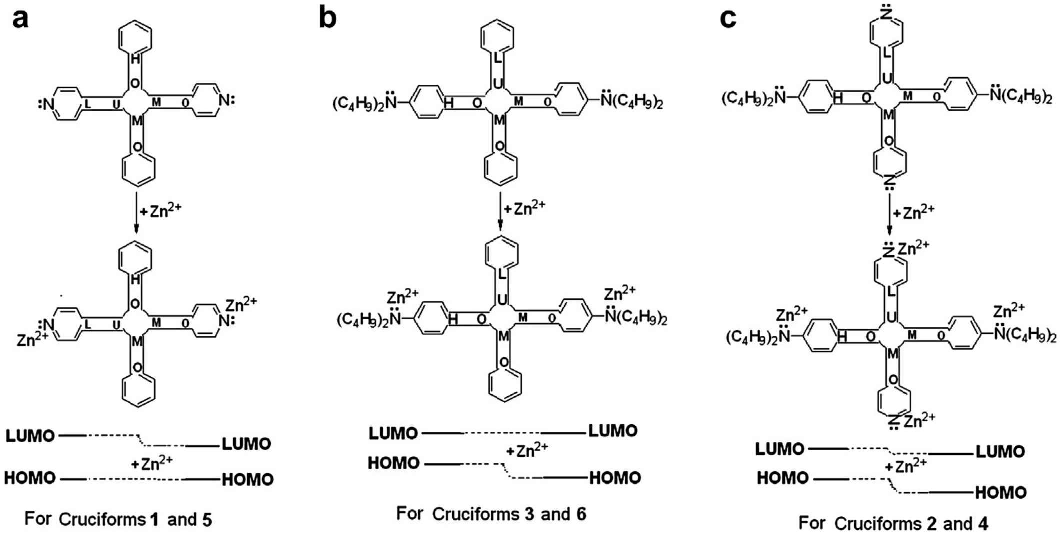

Fig. 7. Schematic diagrams of the changes in energy levels of FMOs for cruciforms **1**–**6** upon coordination with metal ions.

be greater than that of LUMO, which is qualitatively consistent with that the donor segment (dibutylaniline) is more basic than the acceptor pyridine [42].

4. Conclusions

We have demonstrated that 2,6,9,10-tetra(arylvinyl)anthracene cruciforms end-capped with dibutylaniline and/or pyridine exhibit spatially separated frontier molecular orbital features and strong intermolecular charge transfer effect. These anthracene-centered cruciforms have only sensing abilities to transition metal ions such as Zn^{2+} and Cu^{2+}, but they do not respond to alkali and alkaline-earth ions, such as K^{+} and Mg^{2+} and Ca^{2+}. Moreover, the emission shifts upon titration of transition metal ions are monotonous even for those anthracene-centered cruciforms with two different coordination terminals. These fluorescence responsive behaviors to metal ions have been rationalized by qualitatively examining relative energy levels of the FMOs as the coordination happens. Compared with the sensing properties of the benzene-centered analogues to metal ions, it is concluded that the different type of π-centers and molecular symmetry might endow the cruciforms with different optical properties and practical applications.

Acknowledgments

We thank the NSF of China (no. 51173092, 51073083), NSF of Shandong Province (no. ZR2010EM023, ZR2012-EMQ003), and Open Project of State Key Laboratory of Supramolecular Structure and Materials of Jilin University (no. SKLSSM201310).

References

[1] Zucchero A, McGrier P, Bunz U. Cross-conjugated cruciform fluorophores. Acc Chem Res 2010;43(3):397–408.

[2] Wang H, Feng J, Wen G, Jiang H, Wan J, Zhu R, et al. Cruciform p–n diblock conjugated oligomers for electroluminescent applications. New J Chem 2006;30:667–70.

[3] Wang H, Wan J, Jiang H, Wen G, Feng J, Zhang Z, et al. Synthesis and characterization of cross-shaped p–n diblock oligomers. J Polym Sci Part A: Polym Chem 2007;45:1066–73.

[4] Mangalum A, Smith R. Bifunctional cross-conjugated luminescent phosphines and phosphine derivatives: phospha-cruciforms. Dalton Trans 2010;39:5145–51.

[5] Marsden J, Miller J, Shirtcliff L, Haley M. Structure-property relationships of donor/acceptor-functionalized tetrakis (phenylethynyl) benzenes and bis (dehydrobenzoannuleno) benzenes. J Am Chem Soc 2005;127(8):2464–76.

[6] Zhao C, Wakamiya A, Inukai Y, Yamaguchi S. Highly emissive organic solids containing 2,5-diboryl-1,4-phenylene unit. J Am Chem Soc 2006;128:15934–5.

[7] Cui W, Fu Y, Qu Y, Tian H, Zhang J, Xie Z, et al. X- and H-shape two dimensional conjugated oligomers with anthracene as the node. Chem Asian J 2010;5:932–40.

[8] Zhang Z, Xu B, Su J, Shen L, Xie Y, Tian H. Color-tunable solid-state emission of 2,2′-biindenyl-based fluorophores. Angew Chem Int Ed 2011;50:11654–7.

[9] Jin Y, Xu Y, Liu Y, Wang L, Jiang H, Li X, et al. Synthesis of novel diketopyrrolopyrrole-based luminophores showing crystallization-induced emission enhancement properties. Dyes Pigm 2011;90:311–8.

[10] Li J, Duan Y, Li Q. Novel thieno-[3,4-b]-pyrazine derivatives for non-doped red organic light-emitting diodes. Dyes Pigm 2013;96:391–6.

[11] Mangalum A, Gilliard R, Hanley J, Parker A, Smith R. Metal ion detection by luminescent 1,3-bis(dimethylaminomethyl) phenyl receptor-modified chromophores and cruciforms. Org Biomol Chem 2010;8:5620–7.

[12] Davey E, Zucchero A, Trapp O, Bunz U. Discrimination of organic acids using a three molecule array based upon cruciform fluorophores. J Am Chem Soc 2011;133:7716–8.

[13] Parker C, Wei Z, Arroyo C, Jennum K, Li T, Santella M, et al. A new class of extended tetrathiafulvalene cruciform molecules for molecular electronics with, dithiafulvene-4,5-dithiolate anchoring groups. Adv Mater 2013;25:405–9.

[14] Wright I, Kanibolotsky A, Cameron J, Tuttle T, Skabara P, Coles S, et al. Oligothiophene cruciform with a germanium spiro center: a promising material for organic photovoltaics. Angew Chem Int Ed 2012;124:4640–5.

[15] Patze C, Broedner K, Rominger F, Trapp O, Bunz U. Aldehyde cruciforms: dosimeters for primary and secondary amines. Chem Eur J 2011;17:13720–5.

[16] McGrier P, Solntsev K, Zucchero A, Miranda O, Rotello V, Tolbert L, et al. Hydroxydialkylamino cruciforms: amphoteric materials with unique photophysical properties. Chem Eur J 2011;17:3112–9.

[17] Brombosz S, Zucchero A, Phillips R, Vazquez D, Wilson A, Bunz U. Terpyridine-based cruciform-Zn^{2+} complexes as anion-responsive fluorophores. Org Lett 2007;9(22):4519–22.

[18] Zucchero A, Wilson J, Bunz U. Cruclforms as functional fluorophores: response to protons and selected metal ions. J Am Chem Soc 2006;128:11872–81.

[19] Schwaebel T, Schäfer V, Wenz J, Coombs B, Tolosa J, Bunz U. Imine formation as a simple reaction to construct copper-reactive cruciform fluorophores. J Org Chem 2013;78(3):960–5.

[20] Wilson J, Bunz U. Switching of intramolecular charge transfer in cruciforms: metal ion sensing. J Am Chem Soc 2005;127:4124–5.

[21] Schwaebel T, Trapp O, Bunz U. Digital photography for the analysis of fluorescence responses. Chem Sci 2013;4:273–81.

[22] Zhang H, Guo E, Zhang Y, Ren P, Yang W. Donor–acceptor-substituted anthracene-centered cruciforms: synthesis, enhanced two-photon absorptions, and spatially separated frontier molecular orbitals. Chem Mater 2009;21:5125–35.

[23] Li X, Zhang X, Li W, Wang Y, Liu T, Zhang B, et al. Synthesis and enhanced two-photon absorption properties of tetradonor-containing anthracene-centered 2-D cross-conjugated polymers. J Mater Chem 2011;21:3916–24.

[24] Xing L, Yang B, Wang X, Wang J, Chen B, Wu Q, et al. Probing the hydrophobic interactions of a series of pyrene end-labeled poly(ethylene oxide)s in aqueous solution using time-resolved fluorescence. Langmuir 2013;29:2843–8.

[25] Slepkov A, Hegmann F, Tykwinski R, Kamada K, Ohta K, Marsden J, et al. Two-photon absorption in two dimensional conjugated quadrupolar chromophores. Opt Lett 2006;31:3315–7.

[26] Rumi M, Pond S, Friendrichsen T, Zhang Q, Bishop M, Zhang Y, et al. Tetrastyrylarene derivatives: comparison of one- and two-photon spectroscopic properties with distyrylarene analogues. J Phys Chem C 2008;112:8061–71.

[27] Huang F, Tian Y, Chen C, Cheng Y, Young A, Jen A. Cross-conjugated polymers with large two-photon absorption cross-sections for metal ion sensing. J Phys Chem C 2007;111:10673–81.

[28] Wei Z, Li T, Jennum K, Santella M, Bovet N, Hu W, et al. Molecular junctions based on SAMs of cruciform oligo(phenylene ethynylene)s. Langmuir 2012;28:4016–23.

[29] Grunder S, Huber R, Horhoiu V, González M, SchÖnenberger C, Calame M, et al. New cruciform structures: toward coordination induced single molecule switches. J Org Chem 2007;72:8337–44.

[30] Klare J, Tulevski G, Sugo K, Picciotto A, White K, Nuckolls C. Cruciform π-systems for molecular electronics applications. J Am Chem Soc 2003;125:6030–1.

[31] Kumpf J, Bunz U. Aldehyde-appended distyrylbenzenes: amine recognition in water. Chem Eur J 2012;18:8921–4.

[32] Lima J, Miljanić O. Benzobisoxazole fluorophore vicariously senses amines, ureas, anions. Chem Commun 2012;48:10301–3.

[33] Lim J, Nam D, Miljanić O. Identification of carboxylic and organoboronic acids and phenols with a single benzobisoxazole fluorophore. Chem Sci 2012;3:559–63.

[34] Zhang X, Li W, Li X, Liu T, Fan Z, Yang W. Alternating copolymers of 2,6-bis(*p*-dihexylaminostyryl)anthracene-9,10-diyl and *N*-octylcarbazole with large two-photon cross sections. J Polym Sci Part A Polym Chem 2010;48:5704–11.

[35] Li J, Liu T, Zheng M, Sun M, Zhang D, Zhang H, et al. Dibutylaminophenyl- and/or pyridinyl-capped 2,6,9,10-tetravinylanthracene cruciforms: synthesis and aggregation-enhanced one- and two-photon excited fluorescence. J Phys Chem C 2013;117:8404–10.

[36] Tânia M, Carla Q, Rita F, Andreia L, Paula G, Ana M, et al. Design of a water soluble 1,8-naphthalimide/3-hydroxy-4-pyridinone conjugate: investigation of its spectroscopic properties at variable pH and in the presence of Fe^{3+}, Cu^{2+} and Zn^{2+}. Dyes Pigm 2013;98:201–11.

[37] Caroline H, Sylvain A, Isabel L, Joaquín C, Julián R. Metal cation complexation studies of 4-arylvinyl-2,6-di(pyridin-2-yl)pyrimidines: effect on the optical properties. Dyes Pigm 2013;97:230–7.

[38] Wang H, Xue L, Yu C, Qian Y, Jiang H. Rhodamine-based fluorescent sensor for mercury in buffer solution and living cells. Dyes Pigm 2011;91:350–5.

[39] Yin S, Zhang J, Feng H, Zhao Z, Xu L, Qiu H, et al. Zn^{2+}-selective fluorescent turn-on chemosensor based on terpyridine-substituted siloles. Dyes Pigm 2012;95:174–9.

[40] Zou Q, Li X, Zhang J, Zhou J, Sun B, Tian H. Unsymmetrical diarylethenes as molecular keypad locks with tunable photochromism and fluorescence via Cu^{2+} and CN^{-} coordinations. Chem Commun 2012;48:2095–7.

[41] Demas J, Crosby G. The measurement of photoluminescence quantum yields. J Phys Chem 1971;75:991–1024.

[42] Spitler E, Shirtcliff L, Haley M. Systematic structure-property investigations and ion-sensing studies of pyridine-derivatized donor/acceptor-functionalized tetrakis(arylethynyl)benzenes. J Org Chem 2007;72:86–96.